



## OPEN ACCESS

## EDITED BY

Vijay Raghunathan,  
King Mongkut's University of Technology North  
Bangkok, Thailand

## REVIEWED BY

Seyed Borhan Mousavi,  
Texas A and M University, United States  
Mladen Radojković,  
University of Priština in Kosovska Mitrovica,  
Serbia

## \*CORRESPONDENCE

Tomoko Hirayama,  
✉ tomoko@me.kyoto-u.ac.jp

RECEIVED 09 April 2025

ACCEPTED 20 May 2025

PUBLISHED 30 May 2025

## CITATION

Gu H and Hirayama T (2025) Effect of surfactant self-assembly on lubrication performance in oil-based systems: the role of reverse micelles and vesicles.

*Front. Mech. Eng.* 11:1608716.

doi: 10.3389/fmech.2025.1608716

## COPYRIGHT

© 2025 Gu and Hirayama. This is an open-access article distributed under the terms of the [Creative Commons Attribution License \(CC BY\)](https://creativecommons.org/licenses/by/4.0/). The use, distribution or reproduction in other forums is permitted, provided the original author(s) and the copyright owner(s) are credited and that the original publication in this journal is cited, in accordance with accepted academic practice. No use, distribution or reproduction is permitted which does not comply with these terms.

# Effect of surfactant self-assembly on lubrication performance in oil-based systems: the role of reverse micelles and vesicles

Haiyang Gu and Tomoko Hirayama\*

Department of Mechanical Engineering and Science, Graduate School of Engineering, Kyoto University, Kyoto, Japan

Surfactants are effective additives for oil-based lubricants, capable of reducing friction under boundary lubrication conditions through their self-assembly into nanostructures. Understanding the relationship between their self-assembled structures and lubrication properties is essential for optimizing performance. In this study, the aggregation behavior of  $C_{12}E_4$  in dodecane and its effects on friction and anti-wear properties were investigated. The results showed that  $C_{12}E_4$  formed small reverse micelles at lower water concentrations, transitioning to larger reverse vesicles at higher concentrations. Elevated temperatures caused vesicle collapse, leading to the formation of smaller aggregates. Small reverse micelles effectively reduced friction and wear, while larger vesicles increased friction due to their obstructive effect. At higher temperatures, friction coefficients converged as reverse vesicles ruptured under shear. Neutron reflectometry (NR) revealed a strong correlation between the density of the adsorbed layer and frictional properties. As a powerful technique, NR enables direct, nanometer-scale characterization of adsorption layers formed by lubricant additives at solid–liquid interfaces, providing critical insights into the structural basis of lubrication performance. These findings underscore the pivotal role of surfactant self-assembly in oil-based lubrication and highlight the importance of optimizing water content and temperature to achieve effective friction reduction. They offer valuable guidance for developing surfactant-based lubricant additives, particularly for enhancing boundary lubrication performance under high-load and high-temperature industrial conditions.

## KEYWORDS

reverse micelles, reverse vesicles, coefficient of friction, surfactant self-assembly, boundary lubrication

## 1 Introduction

Lubrication is a fundamental element in mechanical systems and plays a key role in reducing friction and wear between interacting surfaces. Effective lubrication improves energy efficiency, extends equipment life and prevents surface damage, making it indispensable in all types of industrial and engineering applications (George et al., 2022). According to the Stribeck curve, in high speed and low load conditions, due to the formation of a complete fluid oil film, the coefficient of friction is low; when the speed of motion is reduced or the load is increased, the oil film gradually becomes thinner, the system enters the mixed lubrication state, at this time the coefficient of friction begins to rise; and in the low-speed or high load and other extreme conditions, it is difficult to maintain the oil

film, the direct contact of the metal is increased, the coefficient of friction increases significantly, and the system enters the boundary lubrication zone (Jacobson, 2003).

Under boundary lubrication conditions, friction and wear problems are particularly severe due to direct contact between metal surfaces and the weakening of traditional oil film protection. This highlights the importance of lubricant additives, especially surface-active organic friction modifiers (OFMs), which are molecules that typically consist of a polar head group that interacts with the surface and a non-polar tail group that is aligned with the lubricant medium. OFM molecules are capable of self-assembling to form a mono- or multimeric layer on a metal surface, which not only reduces the coefficient of friction, but also minimizes direct contact between metal surfaces. This not only effectively reduces the coefficient of friction, but also reduces direct contact between metal surfaces, thereby protecting them and inhibiting wear (Spikes, 2015).

Surfactants are a class of organic friction modifiers (OFMs) with an amphiphilic molecular structure (Apóstolo et al., 2019). When dissolved in water, surfactants can adsorb on air/water surfaces to form well-arranged monolayers, and they can also be enriched at the oil/water interface to reduce the interfacial tension and change the structure and properties of the oil/water interface film. In addition, they can also be adsorbed on solid surfaces to reduce friction and wear. Many studies have been conducted on the use of surfactants as additives to water-based lubricants, and cationic surfactants (Li et al., 2019), anionic surfactants (Zhang and Meng, 2014; He et al., 2010), and nonionic surfactants (Nunes et al., 2014) have been shown to have a low-friction effect. Some studies have also shown that surfactants used as water-based modifiers have better lubricating effects (Wen et al., 2020; Jiang et al., 2022).

As OFMs, surfactants are not only capable of forming monomolecular or multimolecular layers at interfaces, but also nanostructures such as micelles and vesicles through self-assembly. In our previous study, we explored the aggregation behavior of the surfactant 2-hexyldecanoic acid sodium (2HDNa) in aqueous solution and its effect on tribological properties. We found that 2HDNa formed vesicles at low concentrations and transformed into micelles at high concentrations. The presence of vesicles significantly reduces the coefficient of friction and improves the anti-wear performance, while micelles at high concentrations lead to a rebound in the coefficient of friction. Neutron reflection experiments show that vesicles can adsorb and rupture on metal surfaces to form a stable bilayer (~3.01 nm thick), thus reducing direct contact and wear. Thus, the central role of vesicles in water-based lubrication systems is to reduce friction and optimize lubrication performance through the formation of adsorbed films (Gu et al., 2023).

While aqueous lubrication systems offer certain environmental advantages, oil-based lubricants remain predominant in industrial applications due to their superior thermal stability, lower volatility, and better compatibility with mechanical components. The evaporative and corrosive nature of water, along with the instability of aqueous lubrication performance at high temperatures or under high load conditions, further reinforces the reliance on oil-based systems. Therefore, understanding surfactant behavior in oil-based environments is critical for the practical development of effective lubricant additives (Tomala et al.,

2010; Rahman et al., 2021). In water, surfactants typically form self-assembling structures such as conventional micelles or vesicles, in which hydrophilic head groups are oriented toward the water phase and hydrophobic tail groups are clustered in the interior (Perumal et al., 2022). In contrast, in oil-based systems, the self-assembly behavior of surfactants is reversed, with polar head groups located in the interior while the exterior is surrounded by nonpolar solvents, forming reverse micelles and reverse vesicles (Eskici and Axelsen, 2016). Reverse micelles and vesicles in nonpolar solvents have been extensively studied for their structural characteristics. Merdas et al. investigated the temperature dependence of reverse micelles formed by  $C_{12}E_4$  in dodecane, showing that increasing temperature leads to a decrease in micelle size and a transition from spherical to ellipsoidal shapes (Merdas et al., 1996). Kunieda et al. demonstrated that in a water/ $C_{12}E_4$ /dodecane system, reverse vesicles could form at appropriate water contents, emphasizing the critical role of hydration in controlling the aggregate morphology (Kunieda et al., 1991). In addition, Eskici and Axelsen (2016) systematically analyzed the size of AOT reverse micelles in various oils and highlighted how water content and solvent polarity significantly affect micelle dimensions (Eskici and Axelsen, 2016).

Although the self-assembly of surfactants has been extensively studied in aqueous environments, there is a lack of systematic investigation into how reverse micelles and vesicles influence lubrication performance in oil-based systems, particularly under boundary lubrication and thermal conditions. In this study, we investigated the formation of reverse vesicles using surfactant  $C_{12}E_4$  in dodecane and its effect on lubrication performance, with the aim of elucidating how the properties of these self-assembled structures affect the mechanism of friction reduction. We chose  $C_{12}E_4$  because prior studies have demonstrated that  $C_{12}E_4$  can self-assemble to form vesicles in dodecane (Merdas et al., 1996; Kunieda et al., 1991). Its balanced amphiphilic structure and temperature-sensitive aggregation behavior make it an ideal model system for examining the tribological effects of nanostructure transitions. Briefly, the study was driven by the limited understanding of how self-assembled structures such as reverse micelles and vesicles affect boundary lubrication performance in oil-based systems, especially under thermal conditions. Our goal was to fill this knowledge gap and explore the structure–function relationship of surfactants in non-aqueous lubrication. We first studied the self-assembly behavior of  $C_{12}E_4$  in dodecane solution to investigate its lubrication and anti-wear effects. Finally, the adsorbed films were analyzed using a neutron reflectometer. The relationship between the aggregation structure of the surfactant and the lubricating properties in the oil phase was revealed. This study firstly investigate the tribological effects of reverse vesicles in oil-based lubrication systems.

The main contribution of this study lies in the systematic correlation between the self-assembly behavior of a nonionic surfactant in oil-based media and its boundary lubrication performance, evaluated using both macroscopic tribological tests and nanoscale adsorption analysis via neutron reflectometry. In contrast to previous studies that focus on aqueous systems or structural observations alone, this work combines multi-scale characterization to directly link structural transitions to lubrication efficiency. These findings offer a novel perspective on optimizing additive design for non-aqueous lubrication systems.

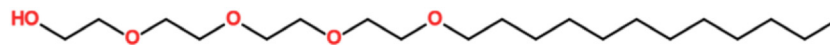


FIGURE 1  
Structure of tetraethylene glycol monododecyl ether ( $C_{12}E_4$ ).

## 2 Experimental

### 2.1 Materials

$C_{12}E_4$  (tetraethylene glycol dodecyl ether, purity  $\geq 98\%$ ) was purchased from Sigma-Aldrich and used without further purification. The molecular structure of  $C_{12}E_4$  is shown in Figure 1. Dodecane (purity  $\geq 99\%$ ) was obtained from Tokyo Chemical Industry and used as the nonpolar solvent. Ultrapure Water was purchased from FUJIFILM Wako Pure Chemical Corporation.

The surfactant solutions were prepared by dissolving 2.5 wt%  $C_{12}E_4$  in dodecane, followed by the addition of water to achieve the desired water concentrations (0.5 wt%, 1.5 wt% and 2.5wt%). To ensure complete dissolution and equilibrium, the samples were ultrasonicated at 25°C for 10 min. The baseline concentration of 2.5 wt%  $C_{12}E_4$  was selected based on previous reports (Merdas et al., 1996; Kunieda et al., 1991), which indicate that this concentration promotes the formation of reverse vesicles in dodecane, enabling investigation of their tribological behavior.

For the neutron reflectometry (NR) experiments, deuterated dodecane (d-dodecane) was used to enhance the contrast between the solvent and the surfactant layer. Deuterated dodecane was obtained from Cambridge Isotope Laboratories, Inc. with a purity of  $\geq 98\%$ .

### 2.2 Dynamic light scattering (DLS)

DLS measurements were performed using a Malvern Zetasizer Nano ZS90 with a 633 nm He-Ne laser at a fixed scattering angle of 90° to determine the hydrodynamic diameter ( $R_h$ ) of the self-assembled structures in the samples. The Zetasizer Nano ZS90 measures hydrodynamic diameters ranging from 1 nm to 3  $\mu\text{m}$  and is particularly suitable for analyzing the size distribution of colloidal aggregates in dilute solutions. Before measurements, the samples were further ultrasonicated for 10 min at the designated measurement temperature (25°C or 50°C). Each DLS measurement was conducted at least three times for each sample to ensure reproducibility. The autocorrelation functions were analyzed using the cumulant method to determine the average hydrodynamic diameter ( $R_h$ ).

### 2.3 Tribology test

Reciprocating tribology tests were carried out using a ball-on-disk type friction tester (FPR-2100, RHESCA Co., Ltd., Japan) under boundary lubrication conditions. The tests were conducted at both room temperature and 50°C to evaluate the effect of temperature on lubrication performance. Temperature was controlled using a built-

in heater with feedback regulation, and monitored continuously via a thermocouple placed near the contact zone. Stainless-steel disks (SUS630, Ra  $\sim 0.04 \mu\text{m}$ , Standard Test Piece Co., Ltd., Japan) with dimensions of 10  $\times$  10  $\times$  2 mm and stainless-steel balls (SUS440C, Ra  $\sim 0.05 \mu\text{m}$ , TSUBAKI NAKASHIMA Co., Ltd., Japan) with diameters of 3/16 inch were used for all experiments.

Prior to testing, both the disks and balls were ultrasonically cleaned in acetone followed by hexane for 5 min to ensure the removal of surface contaminants. Following the cleaning process, 0.1 mL of the prepared sample solution was applied directly to the disk surface. The friction tests were initiated immediately to prevent evaporation or compositional changes in the samples. A normal load of 4.9 N was applied, resulting in an average contact pressure of approximately 820 MPa and a maximum contact pressure of 1.23 GPa according to Hertzian contact theory. These conditions were selected to simulate boundary lubrication environments, reflecting the practical application of surfactant-based additives under high-pressure conditions.

After each tribology test, the contact areas on the stainless-steel balls were analyzed using a 3D measuring laser microscope (OLS4000-SAT, Olympus Co., Japan) to observe and measure the wear scars. The OLS4000-SAT provides non-contact three-dimensional profiling with sub-micrometer lateral resolution, allowing accurate evaluation of wear scar morphology and depth. Each friction and wear test was repeated three times to ensure the reproducibility and reliability of the results.

### 2.4 Neutron reflectometry (NR)

NR is a powerful technique for analyzing the thickness and density of additive layers adsorbed on metal surface (Yamashita et al., 2021; Gu et al., 2025; Gu et al., 2023; Yamashita et al., 2023). NR measurements were performed using the SOFIA horizontal-type neutron reflectometer, located at the Materials and Life Science Experimental Facility of the J-PARC facility (Yamada et al., 2011).

Highly polished silicon blocks (dimensions: 50  $\times$  50  $\times$  10 mm) were used as substrates for NR experiments. The Fe layer ( $\sim 50$  nm thick) was deposited onto polished silicon wafers using the ion beam sputtering facility at the Kyoto University Research Reactor Institute (KUR-IBS) (Hino et al., 2015). The deposition was conducted under an argon atmosphere at a base pressure of  $\sim 5 \times 10^{-5}$  Pa, with a typical rate of  $\sim 0.02$ – $0.03$  nm/s. Sample alignment was carried out automatically using the auto-alignment program on SOFIA, which consists of three main steps: (1) angle scan (rough alignment of the incident angle), (2) height scan (alignment of the sample height), and (3) beam position check (precise alignment of the incident angle). This procedure ensured accurate and stable positioning of the sample during all measurements. To establish a baseline, an initial measurement was conducted with a control sample containing only deuterated dodecane and a reflectivity profile was

obtained. Subsequently, the sample was replaced with solutions containing 2.5 wt%  $C_{12}E_4$ , 2.5 wt%  $C_{12}E_4$  + 0.5 wt%  $H_2O$  and 2.5 wt%  $C_{12}E_4$  + 1.5 wt%  $H_2O$  in deuterated dodecane, and reflectivity profiles were recorded for each condition. The changes in the reflectivity profiles were attributed to variations in the adsorption behavior of the surfactant under different water concentrations. Solution concentrations were controlled with high precision, and samples for comparative measurements were placed in equivalent positions during the same sputtering batch to ensure consistent deposition conditions.

All measurements were conducted at incident angles of  $0.3^\circ$ ,  $0.6^\circ$ , and  $1.2^\circ$ , using a wavelength range of 0.20 nm–0.88 nm. The reflectivity profiles were constructed by merging the data from these different incident angles. The range of momentum transfer perpendicular to the interface,  $Q_z$ , was from 0 to  $0.12 \text{ \AA}^{-1}$ . The neutron irradiation footprint was consistently maintained at  $40 \times 40 \text{ mm}$ . The sample cell and silicon block were firmly secured in a holder throughout the experiment, allowing the solution within the cell to be exchanged without disturbing the relative alignment between the cell and the silicon block.

The reflectivity profiles were analyzed and fitted using GenX 3 software (Glavic and Björck, 2022). The fitting model comprised the Si substrate,  $SiO_2$  layer, Fe layer, FeOx layer, and additive layer. First, the thicknesses and scattering length density (SLD) values of the Si substrate,  $SiO_2$  layer, Fe layer, and FeOx layer were determined by fitting the reflectivity profile of the deuterated dodecane solution. After replacing the solution with the samples containing  $C_{12}E_4$ , the same substrate was used without altering the relative alignment of the sample cell and the silicon block. Therefore, the thicknesses and SLD values of the Si substrate,  $SiO_2$  layer, Fe layer, and FeOx layer remained unchanged. The reflectivity profiles of the samples containing surfactant were then fitted to determine the thickness and SLD values of the additive layer.

Throughout the experimental procedures, several assumptions were made to ensure consistent interpretation of the results. It was assumed that the surfactant self-assembled structures remained stable during sample preparation and handling. The stability of the surfactant during sample preparation and handling was confirmed by monitoring the solutions for up to 1 hour, during which no phase separation or structural changes were observed. All measurements were completed within this period to ensure consistency. Additionally, it was presumed that the observed lubrication behavior was predominantly governed by interfacial phenomena, such as adsorption and aggregation at the sliding interfaces, rather than by bulk fluid properties such as viscosity.

## 3 Results and discussion

### 3.1 Aggregation behavior of $C_{12}E_4$

Figure 2 shows the hydrodynamic diameter ( $R_h$ ) distributions of the  $C_{12}E_4$  system in dodecane at different water concentrations, measured by DLS. In sample (a) (2.5 wt%  $C_{12}E_4$  and 0.5 wt% water), the DLS result exhibits a sharp main peak at approximately 10 nm, indicating the formation of small reverse micelles at low water concentration. The narrow peak suggests a relatively uniform size distribution, consistent with the typical size of reverse micelles

formed by nonionic surfactants in oil. As the water concentration increases to 1.5 wt% (sample b), the DLS result shows a significant increase in the hydrodynamic diameter, with the main peak appearing at approximately 300 nm. The substantial increase in size suggests a structural transition from reverse micelles to larger aggregates. Considering the particle size and sharpness of the peak, this structure is more likely to be an reversed vesicle rather than a swollen reverse micelle or microemulsion, as reverse micelles typically do not exceed 30 nm in size. The relatively narrow peak also indicates a relatively uniform size distribution, which excludes the broad size distribution characteristic of large emulsions, further supporting the formation of reversed vesicles. At a higher water concentration (2.5 wt%, sample c), the main peak in the DLS result shifts back to a smaller size of approximately 20 nm, suggesting that the inverted vesicles formed at intermediate water concentrations may have undergone structural collapse or rearrangement, leading to the formation of smaller reverse micelles. At high water concentrations (2.5 wt%), the osmotic pressure difference between the interior and exterior of the reverse vesicles likely increases, placing stress on the bilayer membrane. Additionally, greater hydration of the polar headgroups may disrupt the packing stability of the bilayer, weakening its structural integrity and promoting collapse or transformation into smaller aggregates such as reverse micelles. Additionally, the secondary peaks observed in the higher  $R_h$  region ( $>1,000 \text{ nm}$ ) in samples (a) and (c) may correspond to a small population of larger aggregates or secondary structures, but their low scattering intensity suggests that these structures are present in minor quantities. Overall, the DLS results indicate that increasing the water concentration induces a transition from small reverse micelles to larger inverted vesicular structures, but at higher water concentrations, these vesicles may undergo reorganization or collapse, forming smaller reverse micelles or aggregates.

### 3.2 Relationship between dissolved structure and coefficient of friction (COF)

The curve of the coefficient of friction with time is shown in Figure 3. The average value of the coefficient of friction for the last 300 s is shown in Figure 4. Under anhydrous conditions (2.5 wt%  $C_{12}E_4$ ), the COF initially decreases rapidly and then stabilizes at approximately 0.102, indicating the formation of a lubricating layer at the interface by reverse micelles. As the water content increases to 0.5 wt%, the COF decreases significantly to slightly below 0.1 and remains stable throughout the experiment. This is consistent with the DLS results, which reveal the formation of small reverse micelles ( $\sim 20 \text{ nm}$ ). The small reverse micelles can adsorb uniformly at the interface, forming a complete and dense lubricating layer that effectively reduces interfacial shear forces, thereby exhibiting optimal lubrication performance. Furthermore, due to their small size ( $\sim 20 \text{ nm}$ ) and flexible aggregation nature, reverse micelles can dynamically rearrange and reconfigure under applied shear. This dynamic behavior enables the formation of a self-healing lubricating layer, allowing the system to maintain a stable low-friction state even under fluctuating load and shear conditions.

When the water content increases to 1–2 wt%, the COF rises to approximately 0.13, indicating a deterioration in lubrication

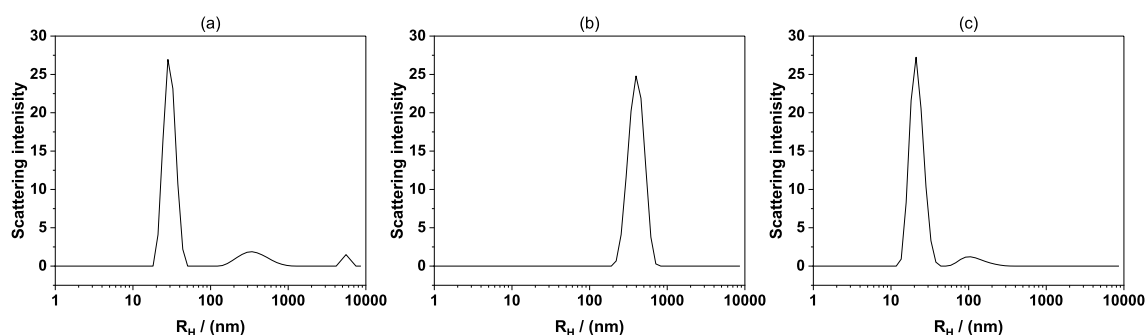


FIGURE 2 Hydrodynamic diameter ( $R_h$ ) distributions measured by DLS of different samples (a) 2.5 wt%  $C_{12}E_4$  and 0.5 wt% water in dodecane, (b) 2.5 wt%  $C_{12}E_4$  and 1.5 wt% water in dodecane, (c) 2.5 wt%  $C_{12}E_4$  and 2.5 wt% water in dodecane.

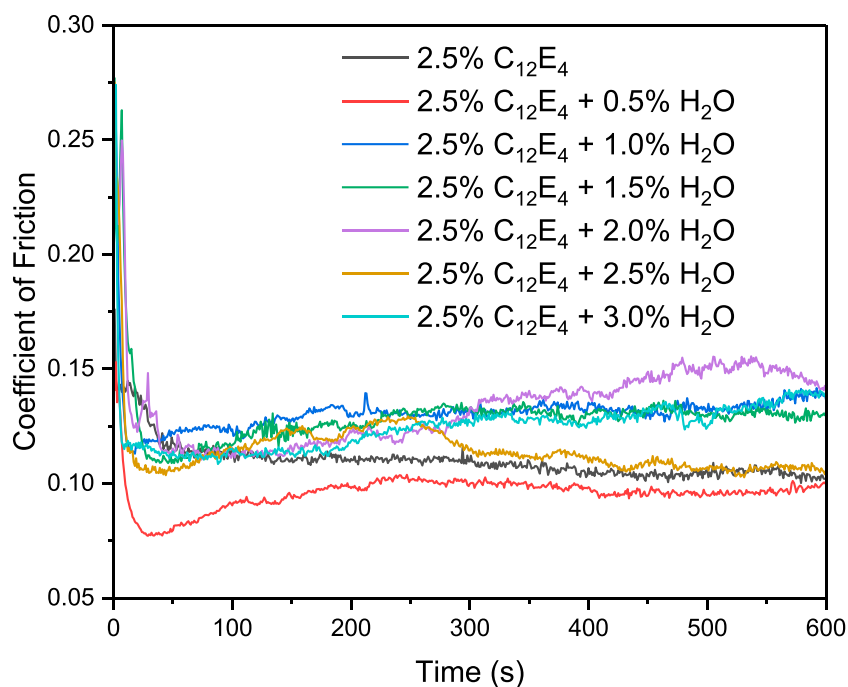


FIGURE 3 Friction coefficient curve for 600 cycles.

performance. This trend aligns with the DLS results, which show the formation of reverse vesicles larger than 100 nm. The larger volume of reverse vesicles may impede the shear process, leading to an increase in the friction coefficient. Further increasing the water content to 2.5 wt% results in a renewed decrease in the COF, which stabilizes at approximately 0.11, superior to the performance at 1.5 wt%. This is consistent with the DLS observation of reverse vesicle collapse and the formation of smaller reverse micelles (~20 nm). The smaller reverse micelles generated by vesicle collapse may form a more flexible and dynamic lubricating layer at the interface, which can more easily reorganize and repair under shear stress, thereby improving lubrication performance.

In terms of wear, Figure 5 shows the microscope images of the ball surface after the friction tests at different water concentrations.

The wear at 0.5 wt% water concentration (Figure 5b) is smaller than that at 0 wt% (Figure 5a). As the water concentration increases to 1–2 wt% (Figures 5c–e), the wear becomes more severe. When the concentration further increases to 2.5–3 wt% (Figures 5f,g), the wear decreases again. Overall, the trend of friction and wear is consistent.

Overall, the friction test results correlate well with the microstructural changes revealed by DLS, indicating that the lubrication performance is directly governed by the aggregation behavior of  $C_{12}E_4$  and water in oil. The best lubrication performance occurs at 0.5 wt% water content, where the small reverse micelles form a complete and stable lubricating layer at the interface. At 1.5 wt% water content, the presence of reverse vesicles hinders the shear process, resulting in a decline in lubrication performance. At 2.5 wt% water content, the collapse of reverse vesicles and the

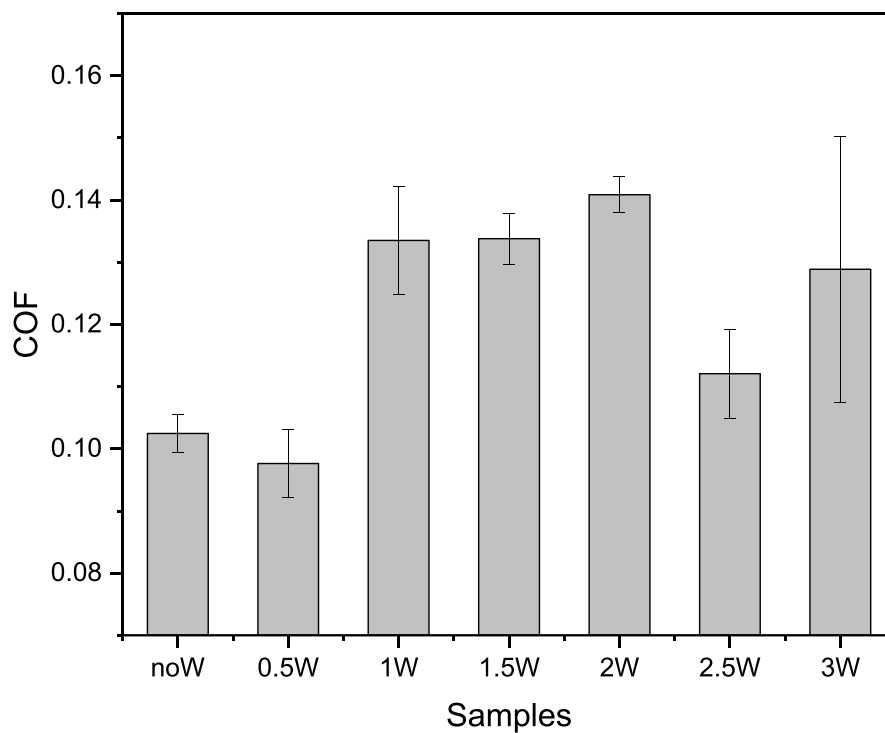


**FIGURE 4** The average value of the coefficient of friction for the last 300 s. The error bars represent the standard deviation of three repeated experiments.

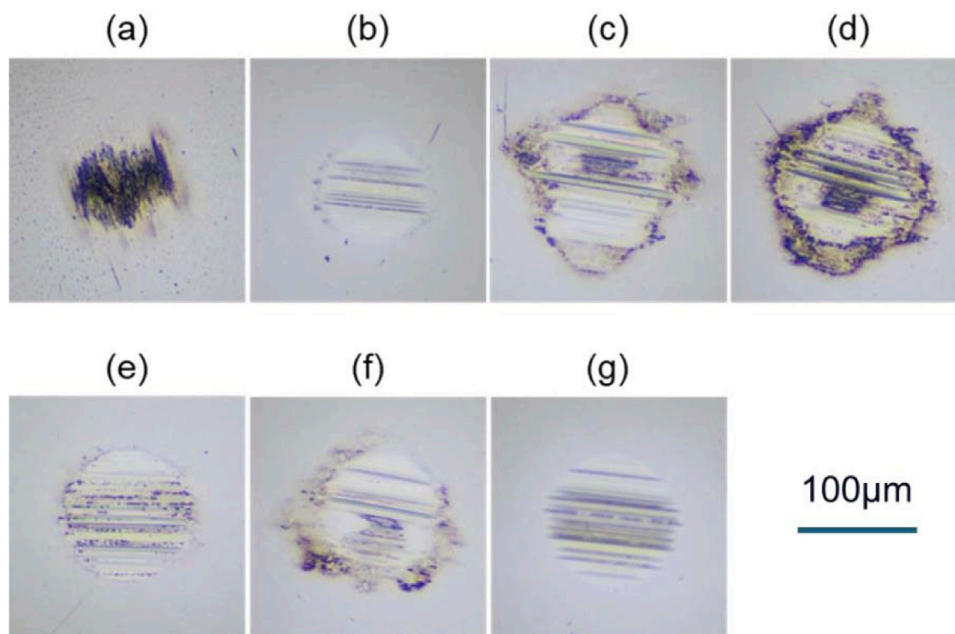


**FIGURE 5** Microscope images of the ball surface after friction tests at different water concentrations. (a–g) Correspond to water concentrations of 0, 0.5, 1, 1.5, 2, 2.5, and 3 wt%, respectively.

formation of smaller reverse micelles facilitate the development of a more flexible lubricating layer, leading to improved friction performance.

In aqueous-based systems, vesicles typically exhibit a low friction coefficient, which may be closely related to their orientation and adsorption behavior at the interface. In water-based systems, vesicles generally adopt an orientation with the hydrophilic head groups facing outward and the hydrophobic tails facing inward. Since metal surfaces typically carry polar functional groups due to oxidation, the polar head groups of vesicles may adsorb onto the metal surface through hydrogen bonding or electrostatic interactions. When vesicles come into contact with a metal surface bearing polar groups, they rupture and form a dense adsorption layer on the surface. In contrast, in oil-based systems, vesicles adopt a structure with non-polar tails facing outward and polar head groups facing inward. This configuration may hinder the adsorption of vesicles onto metal surfaces. Because the outer layer of the vesicle is non-polar, there is a lack of effective adhesive interactions between the vesicles and the polar metal surface. Therefore, reversed vesicles do not spontaneously rupture on the metal surface to form an adsorbed film but remain intact. During the shearing process, they may create a steric hindrance at the interface, resulting in an increased friction coefficient. As a result, the formation of a continuous and stable lubricant film between the contact surfaces is hindered, leading to localized metal-to-metal contacts and contributing to higher friction and wear.

In direct comparison, reverse micelles demonstrated superior lubrication performance, as their small size and flexibility allow them to adsorb uniformly onto the contact interface, forming a continuous and stable lubrication film that reduces shear stress. In contrast, reverse vesicles, with their larger size and lower interfacial adaptability, showed higher friction coefficients. Their bulky structure can create steric hindrance, limiting the formation of a compact adsorbed layer and impeding smooth sliding at the interface. The increased friction observed with reverse vesicles is attributed not only to their large size but also to weaker interfacial interactions. Their non-polar outer layer reduces adsorption affinity for polar metal surfaces, limiting the formation of a stable lubrication film and exacerbating friction through both steric hindrance and poor surface coverage. This comparison underscores the critical role of aggregate size and structural adaptability in determining lubrication efficiency.

### 3.3 Analysis of adsorption layer by neutron reflectometry

Figure 6 illustrates the reflectivity profiles measured by neutron reflectometry, with three samples of different water concentrations selected for measurement. In Figure 6, (a) is a sample without water, (b) is a sample containing 0.5 wt% water, and (c) is a sample containing 1.5 wt% water. In each figure, from top to bottom, the following are represented: base oil containing only deuterated dodecane, samples containing  $C_{12}E_4$  and various concentrations of water, and samples after the test with deuterated dodecane rinse again. The purpose of the post-test rinsing with dodecane was to assess the stability of the adsorbed membrane.

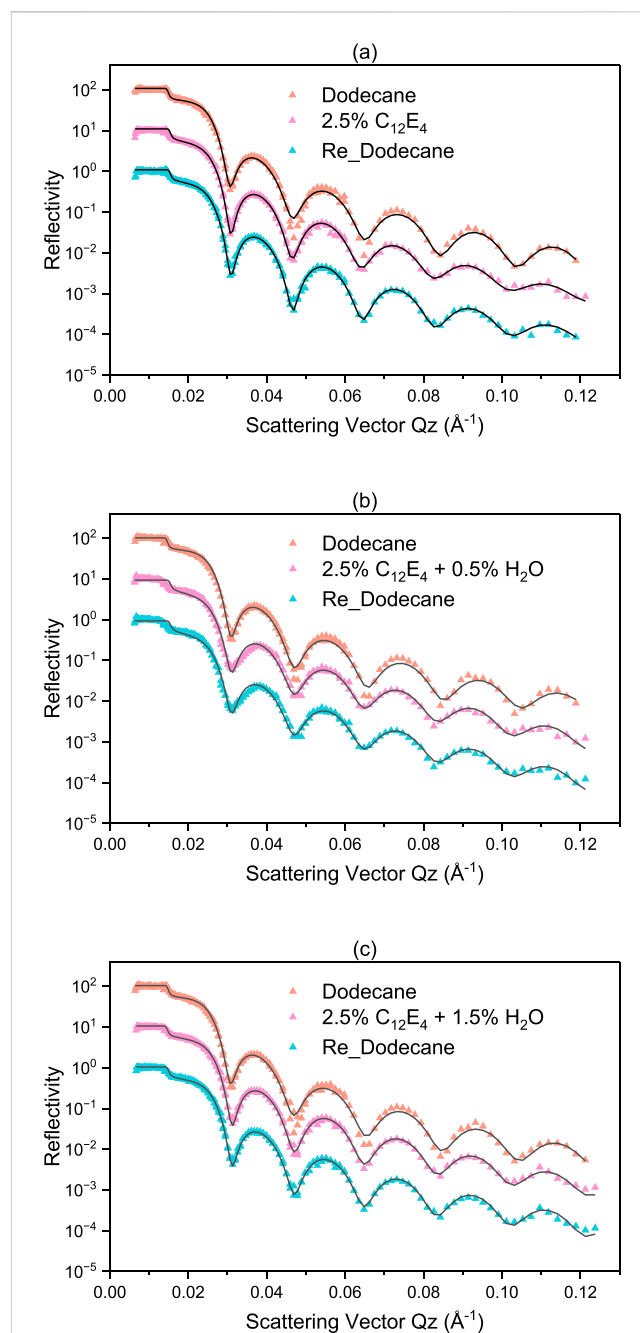


FIGURE 6 Reflectivity profiles for water with different concentration dissolved in deuterated dodecane (a) no water (b) 0.5% and (c) 1.5%. Compared to the sample containing only dodecane, the samples with added surfactant and those rinsed again with dodecane show a noticeable leftward shift in the reflectivity profiles. Compared to the sample containing only dodecane, the samples with added surfactant and those rinsed again with dodecane show a noticeable leftward shift in the reflectivity profiles.

In Figure 6a, the reflection curves of the samples with 2.5 wt%  $C_{12}E_4$  added showed a significant shift to the left compared to the samples containing only dodecane. According to Bragg's law, the shift to the left represents an increase in total thickness. Since the relative position of the cuvette to the substrate remained constant during the experiment, the increase in the total thickness implies the

TABLE 1 Properties of the adsorption layers formed at room temperature: thickness, fitted SLD, and calculated density.

Layer	Thickness (nm)	Fitted SLD [ $10^{-6} \text{ \AA}^{-2}$ ]	Density
2.5% C <sub>12</sub> E <sub>4</sub>	3	2.12	68.4%
2.5% C <sub>12</sub> E <sub>4</sub> + 0.5% H <sub>2</sub> O	3	0.26	96.1%
2.5% C <sub>12</sub> E <sub>4</sub> + 1.5% H <sub>2</sub> O	3	1.58	76.5%

TABLE 2 Properties of the adsorption layers after dodecane rinsing at room temperature: thickness, fitted SLD, and calculated density.

Layer	Thickness (nm)	Fitted SLD [ $10^{-6} \text{ \AA}^{-2}$ ]	Density
2.5% C <sub>12</sub> E <sub>4</sub>	3	3.13	53.4%
2.5% C <sub>12</sub> E <sub>4</sub> + 0.5% H <sub>2</sub> O	3	1.05	84.4%
2.5% C <sub>12</sub> E <sub>4</sub> + 1.5% H <sub>2</sub> O	3	1.51	77.5%

formation of the additive layer. The results in Figure 6b are similar to those in Figure 6a. For the sample containing 2.5 wt% C<sub>12</sub>E<sub>4</sub> and 1.5 wt% water (i.e., Figure 6c), the shift of the curve to the left is significantly less compared to the other two samples, indicating a decrease in the total thickness, i.e., a decrease in the thickness of the additive layer.

Table 1 presents the results of the additive layer density obtained through fitting with the GenX3 software. For comparison purposes, the thickness of the additive layer was fixed at 3 nm during the fitting process. The fixed thickness of 3 nm corresponds to the estimated molecular chain length of a single C<sub>12</sub>E<sub>4</sub> molecule. The adsorption film density was calculated as the ratio of the SLD value obtained through actual analysis to the SLD of the pure additive. The analysis results of the additive layer obtained through NR fitting are consistent with the friction test results. Specifically, when the water content is 0.5 wt%, the adsorption film density increases from 68.4% to 96.1% compared to the case without added water, resulting in a denser adsorption layer that leads to a lower friction coefficient. When the water content increases to 1.5 wt%, as mentioned previously, the reverse micelles transform into reverse vesicles, causing the additive film density to decrease to 76.5% and the friction coefficient to increase accordingly.

After completing the above tests, the substrate was rinsed with dodecane and retested to evaluate the stability of the adsorption film under different conditions. Table 2 summarizes the fitting results of the retests, where the film thickness was also fixed at 3 nm. The trends in film density are consistent with those observed in Table 1. The NR results showed that samples dominated by reverse micelles exhibited higher adsorption density on the substrate, which is consistent with the observed lower friction coefficients. In contrast, vesicle-dominated samples demonstrated lower adsorption density, correlating with poorer lubrication performance. This indicates that adsorption density plays a critical role in forming effective boundary lubrication films that minimize friction.

From the perspective of adsorption dynamics, the formation and uniform adsorption of small reverse micelles are crucial for the integrity and stability of the lubrication layer. NR results indicate that small reverse micelles can form a dense adsorption layer at the

interface, thereby effectively reducing shear force and the friction coefficient. In contrast, due to their larger size, reverse vesicles may cause uneven adsorption at the interface, leading to an incomplete lubrication layer, increased interfacial shear resistance, and ultimately, a higher friction coefficient.

### 3.4 Effect of temperature on the structure and tribological properties of reverse vesicles

The previous section discussed that at room temperature, the presence of reverse vesicles typically leads to an increase in the coefficient of friction due to the relatively large size of the vesicles, which hinders the formation of a uniform lubricating layer at the interface. Temperature is known to have a significant influence on the self-assembly behavior of various aggregates. To further investigate the effect of temperature on the structure and frictional properties of reverse vesicles, DLS and friction experiments were conducted on 2.5 wt% C<sub>12</sub>E<sub>4</sub> solutions and 2.5 wt% C<sub>12</sub>E<sub>4</sub> + 1.5 wt% water solutions at 50°C to examine the structural changes of reverse vesicles under elevated temperatures and their impact on lubrication performance. The temperature of 50°C was selected to simulate moderate operating conditions commonly encountered in mechanical systems, such as engines and industrial machinery. This temperature also allows us to evaluate the thermal stability and transformation of self-assembled surfactant structures under practical shear and load conditions.

Figure 7 shows the DLS results of 2.5% C<sub>12</sub>E<sub>4</sub> + 1.5% water in solution at different temperatures. At room temperature, the hydrated diameter of reverse vesicles formed in the 2.5 wt% C<sub>12</sub>E<sub>4</sub> + 1.5 wt% water solution is approximately 300 nm. However, at 50°C, the vesicle size significantly decreases, with the main peak corresponding to a hydrated diameter of approximately 100 nm. This indicates that increasing the temperature causes a reduction in vesicle size. At higher temperatures, the thermal movement of the molecules is enhanced, causing the self-assembled structures formed by the surfactants (e.g., reverse micelles and reverse vesicles) to become unstable. This leads to

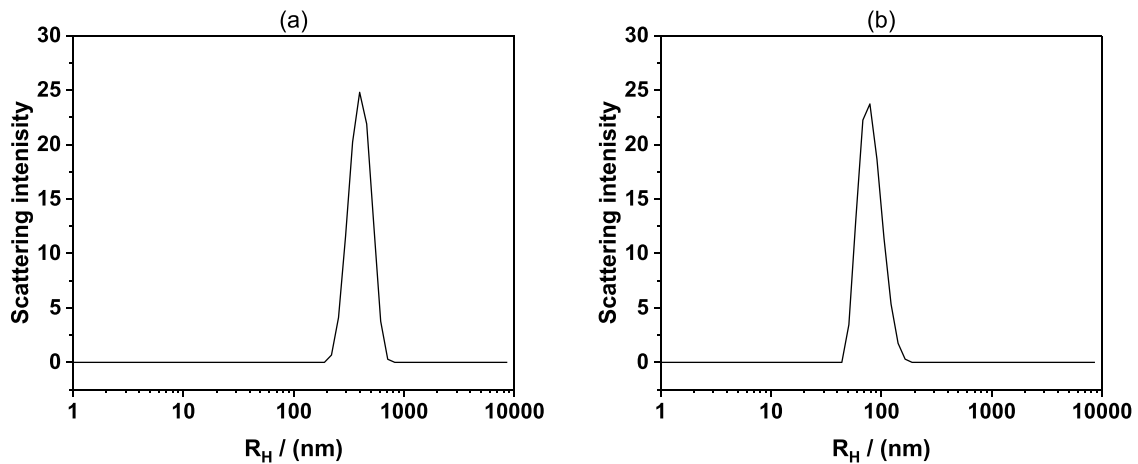


FIGURE 7

Hydrodynamic diameter ( $R_H$ ) distributions measured by DLS for 2.5%  $C_{12}E_4$  + 1.5% water solutions at (a) room temperature and (b) 50°C. The vesicle size decreases from approximately 300 nm at room temperature to around 100 nm at 50°C, indicating that elevated temperature leads to vesicle contraction and structural reorganization.

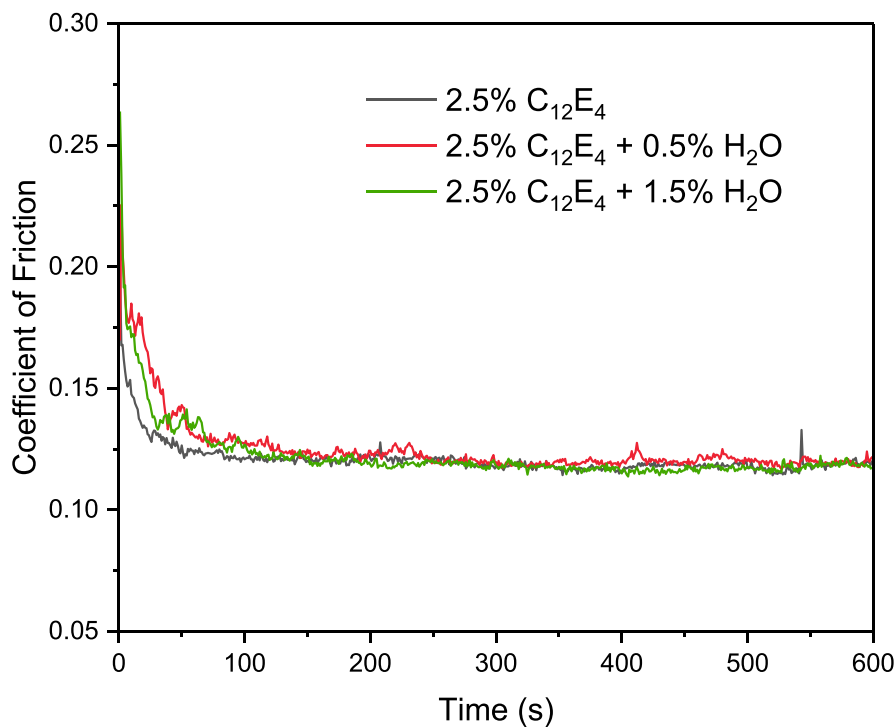


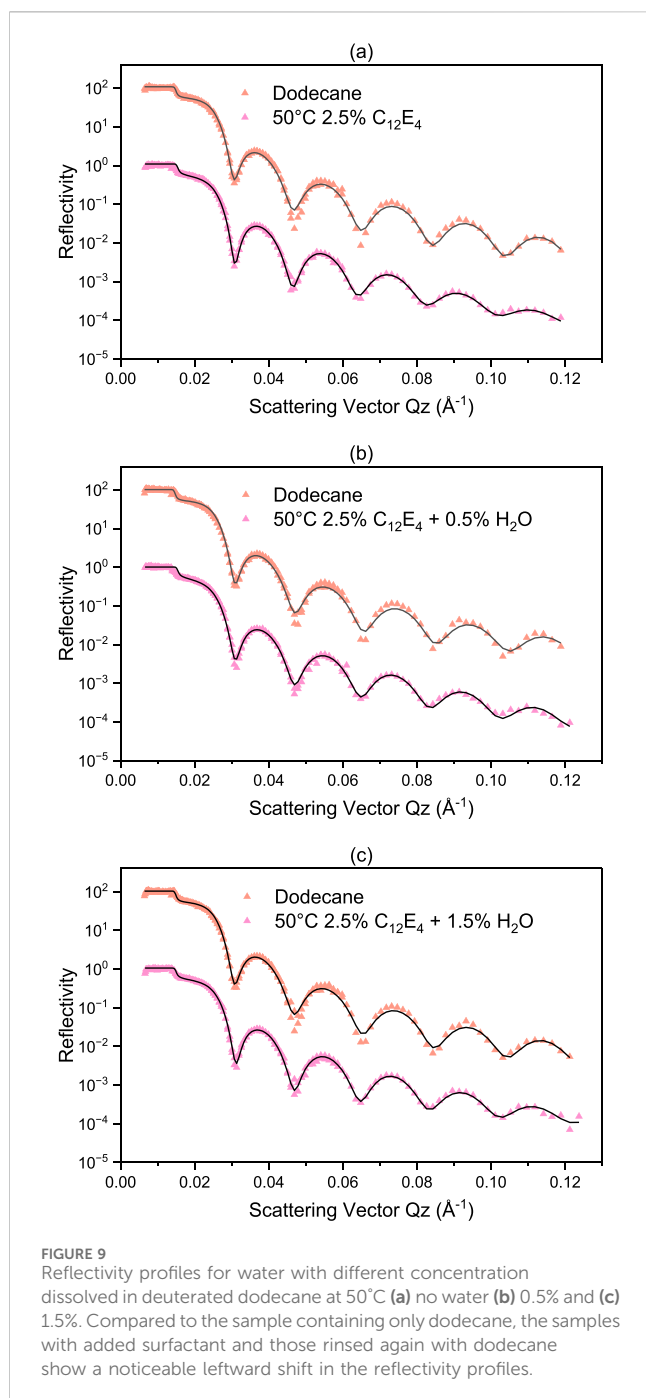
FIGURE 8

Coefficient of friction as a function of time for 2.5 wt%  $C_{12}E_4$  and 2.5 wt%  $C_{12}E_4$  + 1.5 wt% water solutions at 50°C.

the possibility that the reverse vesicles may partially disintegrate or transform into structures of smaller size.

Figure 8 shows the variation of the COF over time at 50°C for the three samples: 2.5 wt%  $C_{12}E_4$ , 2.5 wt%  $C_{12}E_4$  + 0.5 wt%  $H_2O$ , and 2.5 wt%  $C_{12}E_4$  + 1.5 wt%  $H_2O$ . In the steady-state stage, despite some initial differences in COF, the friction coefficients of all three samples eventually stabilized at approximately 0.125. This result suggests that at 50°C, the effect of water content on the friction

coefficient is significantly reduced, leading to a convergence in the friction performance of the different samples. This phenomenon is attributed to elevated temperature promoting the rearrangement of surfactant molecules and the homogenization of the adsorption layer. In addition, the stability of reverse vesicles decreases at high temperatures, causing some vesicles to collapse or reorganize into smaller reverse micelles or monomers, which leads to the convergence of lubrication performance.



It is noteworthy that the DLS results at 50°C did not indicate a complete breakdown of the vesicles into monomers. Considering that DLS measurements were conducted under static, pressure-free conditions, the absence of external forces likely contributed to this difference from the friction experiment results. During the friction test, the high shear forces and contact pressures at the interface caused further disruption and reorganization of the small reverse vesicles, gradually disassembling them into smaller reverse micelles or monomers. These smaller structures could rapidly rearrange under shear, forming a dense and stable lubricating layer at the interface. Consequently, the friction coefficients of the three samples

converged in the steady-state stage, exhibiting performance similar to the sample containing only  $C_{12}E_4$ .

Additional NR experiments were conducted to evaluate the adsorption performance at high temperatures, with the analysis results shown in Figure 9 and Table 3. At 50°C, the film densities of the three samples were 70.49%, 78.09%, and 65.72%, respectively. Although there were still some differences, these differences were significantly reduced compared to those at room temperature.

Another important factor to consider is that the same substrate was used for both the room temperature and high-temperature NR tests. Specifically, the room temperature measurements were completed first, followed by heating to 50°C for the second measurement without altering the state of the substrate or sample. As a result, the initial adsorption state of the sample on the substrate may have influenced the adsorption measurements under high-temperature conditions. Furthermore, unlike the friction experiments, the NR measurements were performed under static conditions without external pressure. In the friction tests, the high shear forces and contact pressure at the interface caused the reverse vesicles to rupture and reorganize into smaller reverse micelles or monomers, forming a dense lubricating layer. In contrast, due to the absence of these external forces during the NR measurements, the reverse vesicles did not undergo further reorganization. Therefore, the measured film density differences partially reflect the structural state of the samples under static conditions.

Nevertheless, the reduced differences in film density among the samples at 50°C suggest that elevated temperatures promote the rearrangement of surfactant molecules and the homogenization of the adsorption layer. This trend of film density convergence across samples is consistent with the observed convergence of the friction coefficients in the friction experiments. These findings further support the conclusion that structural changes in the adsorption layer under high-temperature conditions contribute to the improvement in lubrication performance. Moreover, vesicles may offer potential advantages in applications requiring enhanced load-bearing capacity, encapsulation, or targeted release under specific lubrication conditions. These findings are particularly relevant for high-load and high-temperature industrial lubrication conditions, where controlling the friction coefficient is critical. Notably, the ability of vesicles to increase friction may provide opportunities for tuning frictional properties in specific engineering applications.

These results provide important guidance for the design of surfactant-based additives in oil-based lubrication. The superior performance of reverse micelles highlights the value of promoting small, flexible aggregates that can adsorb uniformly and form stable boundary films. In contrast, additives that tend to form large vesicular structures may be less effective due to limited adsorption and steric hindrance. Understanding these self-assembly behaviors is crucial for developing additives that maintain low friction and wear under demanding operational conditions.

## 4 Summary

In this study, the aggregation behavior of the surfactant  $C_{12}E_4$  in dodecane and its influence on lubrication performance under

TABLE 3 Properties of the adsorption layers formed at 50°C: thickness, fitted SLD, and calculated density.

Layer	Thickness (nm)	Fitted SLD [ $10^{-6} \text{ \AA}^{-2}$ ]	Density
2.5% C <sub>12</sub> E <sub>4</sub>	3	1.98	70.49%
2.5% C <sub>12</sub> E <sub>4</sub> + 0.5% H <sub>2</sub> O	3	1.47	78.09%
2.5% C <sub>12</sub> E <sub>4</sub> + 1.5% H <sub>2</sub> O	3	2.30	65.72%

different water concentrations were investigated. The key findings are summarized as follows:

- DLS results showed that at 0.5 wt% water, small reverse micelles (~20 nm) with a narrow size distribution formed, indicating uniformity and stability. At 1.5 wt% water, the size increased to approximately 300 nm, consistent with the formation of reverse vesicles. At 2.5 wt% water, the size decreased back to ~20 nm, suggesting vesicle collapse and the reformation of smaller reverse micelles.
- Tribology tests demonstrated that small reverse micelles at 0.5 wt% water provided effective lubrication, significantly reducing the friction coefficient and wear. In contrast, at 1.5 wt% water, the formation of large reverse vesicles increased the friction coefficient. The larger vesicles obstructed smooth sliding at the interface, resulting in greater resistance. At 50°C, the friction coefficients of all samples converged to approximately 0.125. This convergence was attributed to the thermal instability of the vesicles, leading to their collapse or reorganization into smaller micelles or monomers under shear, which facilitated the formation of a more uniform and stable lubricating layer.
- NR measurements showed that at room temperature, the adsorption density results aligned with the tribology test findings. The sample with 0.5 wt% water exhibited a higher adsorption density and a lower friction coefficient, while the sample with 1.5 wt% water showed a lower adsorption density and a higher friction coefficient due to the formation of larger reverse vesicles. At high temperatures, the differences in film density among the samples were reduced, indicating enhanced molecular rearrangement and adsorption layer homogenization, further explaining the temperature-induced convergence in friction performance.

Overall, the experimental findings confirmed our initial assumptions that smaller reverse micelles would form more effective lubricating layers. However, the convergence of friction coefficients at high temperature was partially unexpected, suggesting additional thermal effects on aggregate reorganization. These findings provide valuable insights into the self-assembly behavior and lubrication mechanisms of surfactant-based additives in oil-based systems. Understanding the effect of water concentration and temperature on the formation and stability of reverse micelles and vesicles can guide the design of more effective lubrication additives. It should be noted that this study focuses on a single nonionic surfactant (C<sub>12</sub>E<sub>4</sub>) and investigates a limited temperature range, which may restrict the broader applicability of the findings to other surfactant systems or

operational conditions. Future studies could further explore the long-term stability of these self-assembled structures under dynamic conditions and investigate their applicability in real-world industrial applications.

## Data availability statement

The raw data supporting the conclusions of this article will be made available by the authors, without undue reservation.

## Author contributions

HG: Data curation, Methodology, Writing – original draft, Software, Conceptualization, Investigation, Visualization, Validation, Funding acquisition, Supervision, Formal Analysis, Project administration, Resources. TH: Supervision, Funding acquisition, Writing – review and editing, Investigation, Methodology, Conceptualization.

## Funding

The author(s) declare that financial support was received for the research and/or publication of this article. This work was supported by a JSPS DC2 Fellowship (Grant No. 24KJ1406) and JSPS KAKENHI (Grant No. 23H05448).

## Acknowledgments

We sincerely thank Masahiro Hino from the Institute for Integrated Radiation and Nuclear Science at Kyoto University for his generous assistance in preparing the Fe films used for the neutron reflectometry measurements.

## Conflict of interest

The authors declare that the research was conducted in the absence of any commercial or financial relationships that could be construed as a potential conflict of interest.

## Generative AI statement

The authors declare that no Generative AI was used in the creation of this manuscript.

## Publisher's note

All claims expressed in this article are solely those of the authors and do not necessarily represent those of their affiliated

organizations, or those of the publisher, the editors and the reviewers. Any product that may be evaluated in this article, or claim that may be made by its manufacturer, is not guaranteed or endorsed by the publisher.

## References

- Apóstolo, R. F. G., Tsagkaropoulou, G., and Camp, P. J. (2019). Molecular adsorption, self-assembly, and friction in lubricants. *J. Mol. Liq.* 277, 606–612. doi:10.1016/j.molliq.2018.12.099
- Eskici, G., and Axelsen, P. H. (2016). The size of AOT reverse micelles. *J. Phys. Chem. B* 120 (44), 11337–11347. doi:10.1021/acs.jpcc.6b06420
- George, S. C., Haponiuk, J. T., Thomas, S., Reghunath, R., and Sarath, P. S. (2022). *Tribology of polymers, polymer composites, and polymer nanocomposites*. Elsevier.
- Glavic, A., and Björck, M. (2022). GenX 3: the latest generation of an established tool. *J. Appl. Crystallogr.* 55 (4), 1063–1071. doi:10.1107/S1600576722006653
- Gu, H., Hirayama, T., Yamashita, N., Okano, T., Xu, J., Sato, N., et al. (2023). Tribological performance of a surfactant derived from its structure of molecular aggregates in water. *Tribol. Int.* 188 (October), 108881. doi:10.1016/j.triboint.2023.108881
- Gu, H., Hirayama, T., Yamashita, N., Xu, J., and Yamada, M. (2025). Relationship between friction reduction effect and solubility in base oil of organic friction modifiers. *Tribol. Int.* 202 (February), 110304. doi:10.1016/j.triboint.2024.110304
- He, S., Meng, Y., Tian, Y., and Zuo, Y. (2010). Response characteristics of the potential-controlled friction of ZrO<sub>2</sub>/stainless steel tribopairs in sodium dodecyl sulfate aqueous solutions. *Tribol. Lett.* 38 (2), 169–178. doi:10.1007/s11249-010-9587-3
- Hino, M., Oda, T., Kitaguchi, M., Yamada, N. L., Tasaki, S., and Kawabata, Y. (2015). The ion beam sputtering facility at KURRI: coatings for advanced neutron optical devices. *Nucl. Instrum. Methods Phys. Res. Sect. A Accel. Spectrom. Detect. Assoc. Equip.* 797 (October), 265–270. doi:10.1016/j.nima.2015.06.046
- Jacobson, Bo (2003). The Stribeck memorial lecture. *Tribol. Int.* 36 (11), 781–789. doi:10.1016/S0301-679X(03)00094-X
- Jiang, H., Hou, X., Ma, Y., Su, D., Qian, Y., Ali, M. K. A., et al. (2022). The tribological performance evaluation of steel-steel contact surface lubricated by polyalphaolefins containing surfactant-modified hybrid MoS<sub>2</sub>/h-BN nano-additives. *Wear* 504-505 (September), 204426. doi:10.1016/j.wear.2022.204426
- Kunieda, H., Nakamura, K., Davis, H. T., and Fennell Evans, D. (1991). Formation of vesicles and microemulsions in a water/tetraethylene glycol dodecyl ether/dodecane system. *Langmuir* 7 (9), 1915–1919. doi:10.1021/la00057a016
- Li, J., Li, J., Jiang, L., Chen, X., and Luo, J. (2019). Cationic surfactant micelles lubricate graphitic surface in water. *Langmuir* 35 (34), 11108–11113. doi:10.1021/acs.langmuir.9b01804
- Merdas, A., Gindre, M., Ober, R., Nicot, C., Urbach, W., and Waks, M. (1996). Nonionic surfactant reverse micelles of C12E4 in dodecane: temperature dependence of size and shape. *J. Phys. Chem.* 100 (37), 15180–15186. doi:10.1021/jp960628p
- Nunes, D. G., da Silva, A. P. M., Cajaiba, J., Pérez-Gramatges, A., Lachter, E. R., and Nascimento, R. S. V. (2014). Influence of glycerides-xanthan gum synergy on their performance as lubricants for water-based drilling fluids. *J. Appl. Polym. Sci.* 131 (22). doi:10.1002/app.41085
- Perumal, S., Atchudan, R., and Lee, W. (2022). A review of polymeric micelles and their applications. *Polymers* 14 (12), 2510. doi:10.3390/polym14122510
- Rahman, Md H., Warneke, H., Webbert, H., Rodriguez, J., Austin, E., Tokunaga, K., et al. (2021). Water-based lubricants: development, properties, and performances. *Lubricants* 9 (8), 73. doi:10.3390/lubricants9080073
- Spikes, H. (2015). Friction modifier additives. *Tribol. Lett.* 60 (1), 5. doi:10.1007/s11249-015-0589-z
- Tomala, A., Karpinska, A., Werner, W. S. M., Olver, A., and Störi, H. (2010). Tribological properties of additives for water-based lubricants. *Wear* 269 (11), 804–810. doi:10.1016/j.wear.2010.08.008
- Wen, P., Lei, Y., Li, W., and Fan, M. (2020). Synergy between covalent organic frameworks and surfactants to promote water-based lubrication and corrosion resistance. *ACS Appl. Nano Mater.* 3 (2), 1400–1411. doi:10.1021/acsanm.9b02198
- Yamada, N. L., Torikai, N., Mitamura, K., Sagehashi, H., Sato, S., Seto, H., et al. (2011). Design and performance of horizontal-type neutron reflectometer SOFIA at J-PARC/MLF. *Eur. Phys. J. Plus* 126 (11), 108. doi:10.1140/epjp/i2011-11108-7
- Yamashita, N., Hirayama, T., Hino, M., and Yamada, N. L. (2023). Neutron reflectometry under high shear in narrow gap for tribology study. *Sci. Rep.* 13 (1), 18268. doi:10.1038/s41598-023-45161-9
- Yamashita, N., Hirayama, T., Yamada, N. L., Watanabe, H., Onodera, K., and Sato, T. (2021). Highly swollen adsorption layer formed by polymeric friction modifier providing low friction at higher temperature. *Tribol. Lett.* 69 (2), 65. doi:10.1007/s11249-021-01443-9
- Zhang, J., and Meng, Y. (2014). Stick-slip friction of stainless steel in sodium dodecyl sulfate aqueous solution in the boundary lubrication regime. *Tribol. Lett.* 56 (3), 543–552. doi:10.1007/s11249-014-0431-z